

# Preparation and Mechanical Properties of Polypropylene/Clay Nanocomposites for Automotive Parts Application

Chae Hwan Hong,<sup>1</sup> Young Bum Lee,<sup>1</sup> Jin Woo Bae,<sup>1</sup> Jae Young Jho,<sup>1</sup> Byeong Uk Nam,<sup>2</sup> Tae Won Hwang<sup>3</sup>

<sup>1</sup>Hyperstructured Organic Materials Research Center and School of Chemical Engineering, Seoul National University, Kwanak-gu, Seoul 151-742, Korea

<sup>2</sup>Department of Applied Chemical Engineering, Korea University of Technology and Education, Chungnam 330-708, Korea

<sup>3</sup>Polymeric Materials Research Team, Research & Development Division for Hyundai Motor Company & Kia Motor Company, Kyunggi, Korea

Received 16 January 2005; accepted 22 February 2005

DOI 10.1002/app.21800

Published online in Wiley InterScience (www.interscience.wiley.com).

**ABSTRACT:** Nanocomposites of polypropylene with organically modified clays were compounded in a twin-screw extruder by a two-step melt compounding of three components, i.e., polypropylene, maleic anhydride grafted polypropylene (PPgMA), and organically modified clay. The effect of PPgMA compatibilizers, including PH-200, Epolene-43, Polybond-3002, and Polybond-3200, with a wide range of maleic anhydride (MA) content and molecular weight was examined. Nanocomposites' morphologies and mechanical properties such as stiffness, strength, and impact resistance were investigated. X-ray diffraction patterns showed that the dispersion morphology of clay particles seemed to be

determined in the first compounding step and the further exfoliation of clays didn't occur in the second compounding step. As the ratio of PPgMA to clay increased, the clay particles were dispersed more uniformly in the matrix resin. As the dispersibility of clays was enhanced, the reinforcement effect of the clays increased; however, impact resistance decreased. © 2005 Wiley Periodicals, Inc. *J Appl Polym Sci* 98: 427–433, 2005

**Key words:** polypropylene; nanocomposite; clay; stiffness; impact resistance

## INTRODUCTION

Recently polypropylene (PP) has been considered one of the promising materials to replace engineering plastics. To improve polypropylene's competitiveness in engineering resin application, it is necessary to simultaneously increase dimensional stability, heat distortion temperature, stiffness, and impact resistance without sacrificing easy processability. The production of polypropylene composites containing fiber reinforcement requires special processing technology involving fiber impregnation and prepreg formation. Therefore, extensive studies are being performed upon the development of filled polypropylene, which is produced by means of conventional melt processing technology. Traditional fillers for polypropylene are calcium carbonate, talc, glass fiber, wollastonite, mica, glass beads, and wood flour. Filled PP containing talc is used extensively because of a combination of stiffness, dimensional stability, and, importantly, low cost. Filler anisotropy is especially favorable in matrix reinforcement. Although anisotropic nanofillers were

expected to afford attractive combinations of stiffness and toughness, limited commercial availability and dispersion problems due to strong interparticle interactions of nanofillers have limited their application. One of the most common nanoscopic fillers is derived from montmorillonite (MMT) clay, which is found naturally in a layered silicate structure with a high surface area, about 750 m<sup>2</sup>/g. The clay exists in a tactoid structure of 20–25 layers. Exchanging the cations in between the silicate layers with the bulkier and more organophilic cations alters the clay structure known as organoclay. This expansion of the clay layer or basal spacing makes it possible to be intercalated and exfoliated.

Nanocomposites based on organic polymers and inorganic clay materials consisting of silicate layers have attracted a great deal of interest, because they have shown dramatic improvements in mechanical, thermal, and barrier properties with a small amount of layered silicates. A large number of polymer/clay nanocomposites have been studied including polystyrene,<sup>1</sup> polyamide,<sup>2</sup> polyimide,<sup>3</sup> epoxy resin,<sup>4</sup> and polypropylene.<sup>5–20</sup> The dispersion of silicate layers strongly depends on the preparation techniques, such as *in situ* polymerization, solution blending, or melt compounding. In this work, PP/clay nanocomposites are obtained by direct melt compounding of PP with organic MMT in the presence of maleic anhydride-

Correspondence to: Byeong Uk Nam (bunam@kut.ac.kr).

Contract grant sponsor: Hyundai Motor Company, South Korea.

grafted PP (PPgMA). This method was first developed by researchers at Toyota Central R and D Laboratories.<sup>6</sup> They added three times as much PPgMA as the clay by weight in preparing well-mixed PP/clay nanocomposites. Thereafter, the melt compounding intercalation method was recognized as a promising approach because of its ease of employing conventional compounding process, although the successful result of *in situ* polymerization method was reported recently.<sup>9</sup> For nonpolar polymers such as PP, unless the organoclay is further treated with compatibilizers, applying high shear alone during melt compounding does not cause the clay tactoid to delaminate.

Efforts were made to improve both the dispersion of clay in PP matrix by using functional oligomers as compatibilizers and the mechanical properties of clay nanocomposites to use for industrial applications. One of the attractive application fields of clay nanocomposites is automotive parts. The use of nanocomposites in vehicle parts and system is expected to reduce weight and promote recycling. Applying these nanocomposites to structurally noncritical parts such as front and rear fascia, cowl top cover, waist line molding, and valve cover could offer a 25 wt % weight saving on average over highly filled plastics and further energy savings could be expanded into structural components, such as interior parts and body panels. As important as the weight and energy savings are the enhanced physical properties that clay nanocomposites offer, such as stiffness, strength, and dimensional stability.

The objective of this study is to investigate the effect of compatibilizer type and compounding conditions on the clay dispersion in PP matrix and mechanical properties of PP/clay nanocomposites, such as stiffness, strength, and impact resistance for automotive parts application.

## EXPERIMENTAL

### Materials

The matrix PP used for this study was block-PP, which was produced by Polymirae Co., Korea. The grade name is EP641P (density = 0.905 g/cm<sup>3</sup>, melt flow rate = 20 g/10 min at 230°C, 2.16 kg load). Four types of PPgMA containing different amounts of maleic anhydride group were used in this study, PH-200 (containing 2.6 wt % maleic anhydride, supplied by Honam Petrochemical Co.,  $M_w$  = 49,600), Epolene-43 (containing 4.2 wt % maleic anhydride, supplied by Eastman Chemical Co.,  $M_w$  = 18,700), Polybond-3002 (containing 0.2 wt % maleic anhydride, supplied by Crompton, melt flow rate = 7 g/10 min at 230°C, 2.16 kg load), and Polybond-3200 (containing 1.0 wt % maleic anhydride, supplied by Crompton, melt flow rate = 110 g/10 min at 190°C, 2.16 kg load). From the

molecular weight data and melt flow rate data, we can assume that in increasing order of molecular weight, the PPgMA grades are Epolene-43 < PH-200 < Polybond-3200 < Polybond-3002.

The commercial organic modified montmorillonite, Cloisite 20A, supplied by Southern Clay Products, was used and was ion-exchanged with dimethyl di(hydrogenated tallow) ammonium ions (tallow was composed predominantly of dodecyl chains with a smaller amount of lower homologues, e.g., the approximate composition of C<sub>18</sub> 65%, C<sub>16</sub> 30%, and C<sub>14</sub> 5%). Talc used in this study for the preparation of conventional PP/talc microcomposites was a 2- $\mu$ m mineral, BT-2202 from Suzorite.

As an impact modifier for PP/talc conventional microcomposites and PP/clay nanocomposites, metalocene catalyzed polyolefin elastomer (POE) was used. The grade name was Engage 8842 (comonomer content = 45 wt %, density = 0.857 g/cm<sup>3</sup>, melt flow rate = 1.0 g/10 min at 190°C, 2.16 kg load), supplied by DuPont Dow Elastomer. PP is a thermoplastic with a number of desirable properties. However, the poor impact properties, especially at low temperature, limit some of its application. To achieve better properties, impact modifiers have been added to PP. Among the impact modifiers commonly used for PP, POE exhibits the advantage of mechanical properties when blended with PP.<sup>21-27</sup>

### Preparation of PPgMA/clay nanocomposite master batch

In this study, PP/clay nanocomposites were prepared by a two-step compounding process. Prior to preparation of final PP/clay nanocomposites, PPgMA/clay master batches containing 30 and 40 wt % clay were prepared. PPgMA powder or pellet and the clay were premixed in a tumbling mixer together with 0.2 wt % of stabilizer. The mixture was melt-blended in a corotating twin-screw extruder (Werner and Pfleiderer; ZSK 25) at 150–190°C and 150 rpm. The screw consisted of 10 segmented barrels with three kneading zones. The major processing variables were screw speed, barrel temperature profiles, and throughput rate. After several trials, the screw speed was set at 150 rpm and the barrel temperature were set from 150°C at the first barrel to 190°C at the last barrel for the first compounding step. The obtained strands were pelletized and then dried at 80°C for 12 h. The compositions of the master batch samples are summarized in Table I. (The sample names are abbreviated MB-1 to -7)

### Compounding of PPgMA/clay master batch with neat PP

Second, the dried master batch composite pellets obtained in the previous step were premixed with neat block-PP pellets in a tumbling mixer together with 0.2

**TABLE I**  
**Compounding Formulations of the First Compounded Master Batch Composites**  
**and the Second Compounded Final Products**

Formulation code	Block-PP EP641P (wt %)	PH-200 (wt %)	Epolene-43 (wt %)	Polybond -3002 (wt %)	Polybond -3200 (wt %)	Organo Clay (wt %)
<i>First compounding (PPgMA and clay compounding)</i>						
MB-1	—	70	—	—	—	30
MB-2	—	—	70	—	—	30
MB-3	—	—	52.5	17.5	—	30
MB-4	—	—	35	35	—	30
MB-5	—	—	17.5	52.5	—	30
MB-6	—	—	—	—	70	30
MB-7	—	60	—	—	—	40
<i>Second compounding (block-PP and Master Batch(MB) compounding)</i>						
P-1	67	23	—	—	—	10
P-2	—	—	—	—	—	—
P-3	67	—	17.3	5.7	—	10
P-4	67	—	11.5	11.5	—	10
P-5	67	—	5.7	17.3	—	10
P-6	67	—	—	—	23	10
P-7	75	15	—	—	—	10

wt % of stabilizer. For example, sample code P-1 in Table I was made by mixing 70 part neat block-PP with 30 part MB-1, and consequently the clay content of final composite was 10 wt %. The mixtures were melt-blended in a corotating twin-screw extruder (Werner and Pfeleiderer; ZSK 25) at 190–230°C and 300 rpm. In the second compounding step, the screw speed was set at 300 rpm and the throughput rate was 10 kg/h. The obtained strands were pelletized and then dried at 80°C for 12 h. The compositions of the samples are also summarized in Table I (sample code P-1 to -7). The dried pellets were injection-molded into ASTM specimens for mechanical testing. The injection molding machine was a LGH-80D produced by LG Cable Ltd. The temperatures of the machine were 200, 210, and 235°C from hopper to die. The injection pressure and injection speed were 120 MPa and 80 cm<sup>3</sup>/s, respectively. The temperature of the mold was kept at room temperature.

### Clay dispersion analysis

X-ray diffraction (XRD) analysis was carried out using Nanostar, Bruker X-ray diffractometer (CuK $\alpha$  radiation with  $\lambda = 0.15, 406$  nm, generator voltage = 30 kV, current = 45 mA) at room temperature. The diffractogram was scanned in  $2\theta$  ranges from 1.0 to 10° at a rate of 1°/min. Measurement were recorded every 0.03°. For comparative purposes, the XRD patterns were represented in terms of relative intensities; the intensity of the strongest reflection was arbitrarily assigned a value of  $d_{001}$ , the interplanar distance.

Bright field transmission electron microscopy (TEM) images of nanocomposites were obtained at an acceleration voltage of 120 kV operating power with a JEOL

JEM-2000 EXII TEM. The nanocomposite samples, embedded in an epoxy resin and cured at 80°C overnight, were microtomed to give 70-nm-thick sections. Ultrathin sections were prepared with a 45° diamond knife at room temperature using a Leica Ultracut UCT microtome. The sections were transferred from water to carbon-coated Cu grids of 200 mesh. The contrast between the layered silicates and the polymer was sufficient for imaging, so no heavy metal staining of sections prior to imaging was required.

### Mechanical property evaluation

The specimens were prepared and conditioned as per ASTM to analyze various physicochemical properties with testing condition of  $23 \pm 1^\circ\text{C}$  and  $55 \pm 2\%$  RH.<sup>28</sup> Specific gravity of the neat PP and the nanocomposites was measured as per ASTM-D-792. Tensile properties were measured as per ASTM-D-638 with a gauge of 50 mm and cross-head speed of 50 mm/min. Flexural properties were carried out as per ASTM-D-790 with a gauge length of 50 mm and crosshead speed of 1.3 mm/min. Both properties were measured using a Universal Testing Machine (LR 100K Lloyd Instruments Ltd., UK). The notched izod impact strength of the specimens was measured by using Impactometer (Ceast, Italy) with a 2.54-mm notch and 45° notch angle as per ASTM D-256. All mechanical data reported were the average of five tests of the same test for each sample.

## RESULTS AND DISCUSSION

### Structural analysis of nanocomposites

The dispersibilities of the clay layers in the matrix resin were evaluated using XRD and TEM. Figure 1

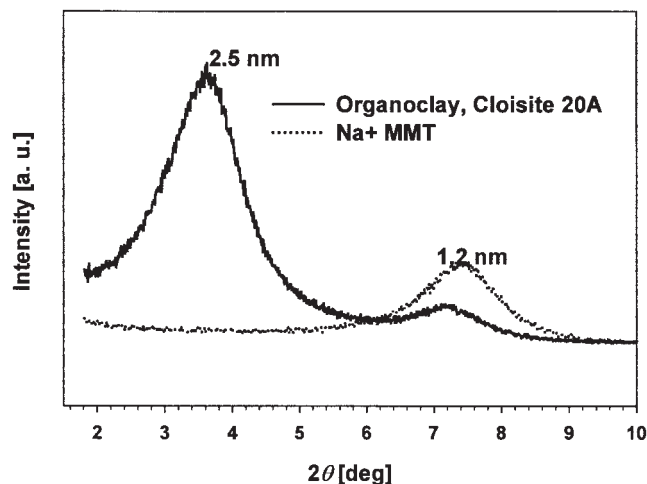


**Figure 1** X-ray diffraction patterns of Na<sup>+</sup> MMT and organic modified MMT, Cloisite 20A.

shows the XRD patterns of Na<sup>+</sup> MMT and organic modified MMT, Cloisite 20A. The latter exhibited two well-defined peaks. The characteristic diffraction peak  $d_{001}$  was located at around 3.4°, corresponding to a basal interlayer spacing of 2.5 nm according to Bragg's equation. Figure 2 shows the XRD patterns of the first compounded master batch composites where peaks correspond to the (001) plane reflections of the clays. Four types of PPgMA containing different amounts of maleic anhydride group were used. In the case of PH-200 containing 2.6 wt % maleic anhydride group (MB-1), there were no peaks in the XRD pattern. In the case of Epolene-43 containing 4.2 wt % maleic anhydride group (MB-2), it was impossible to take strands continuously during the compounding operation in the twin-screw extruder. This was because the molar mass of Epolene-43 was very low and consequently the melt viscosity of that was also very low at this

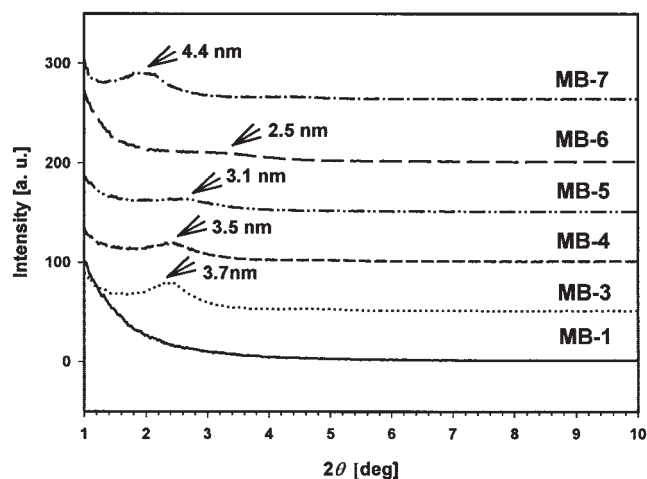


**Figure 2** X-ray diffraction patterns of the first compounded PPgMA/clay master batch nanocomposites.

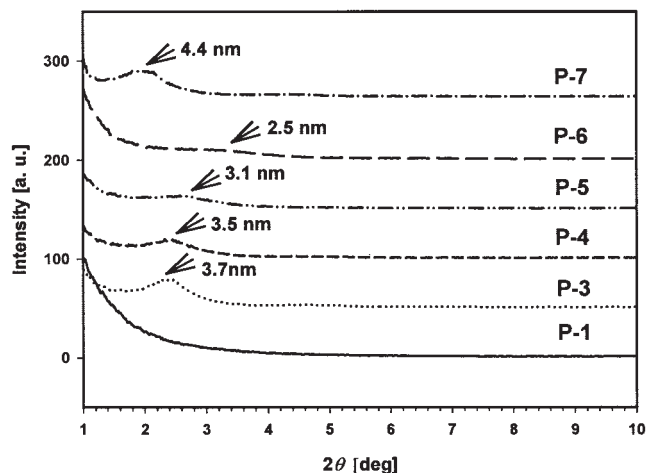


**Figure 3** X-ray diffraction patterns of the second compounded block-PP/master batches (PPgMA/clay nanocomposites) nanocomposites.

compounding condition. In addition, the XRD pattern for MB-2, not shown here, displayed prominent clay peaks. The ineffective compatibilizer in this study, Epolene-43, has a weight average molecular weight of 18,700. This low-molecular-weight matrix resin might be less efficient in transferring the stress from the shear field to the clay during processing. Therefore, to effectively transfer stresses from the polymer melt to the clay in the continuous compounding process, it is thought that the certain minimum molecular weight of compatibilizer is required and PH-200, having a weight average molecular weight of 49,600, is suitable for the compounding operation and the clay dispersion.

To vary the maleic anhydride content in the compatibilizer, we tried to use the mixtures of Epolene-43 and Polybond-3002, having a sufficiently high molecular weight and 0.2 wt % maleic anhydride group. The contents of maleic anhydride group in these mixtures were 2.2 wt % (MB-3), 1.5 wt % (MB-4), and 0.2 wt % (MB-5), respectively, and the continuous compounding operations were possible. The XRD patterns of nanocomposites, MB-3, -4, and -5, exhibited the clay peaks or shoulders. In case of MB-6 prepared using Polybond-3200 containing 1.0 wt % maleic anhydride group, there was a broad clay peak shoulder. From the comparison of XRD patterns of MB-1 and MB-6, it is apparent that maleic anhydride content in the compatibilizer affected the dispersibility of the clays although the shear force exerted by the compatibilizer used in MB-6 was thought to be greater than that used in MB-1. From these results, it will be necessary to consider both the molecular weight and the maleic anhydride content of compatibilizer simultaneously for the PPgMA/clay master batch compounding process.

Figure 3 shows the XRD patterns of the second compounded neat block-PP/MBs composites. In com-

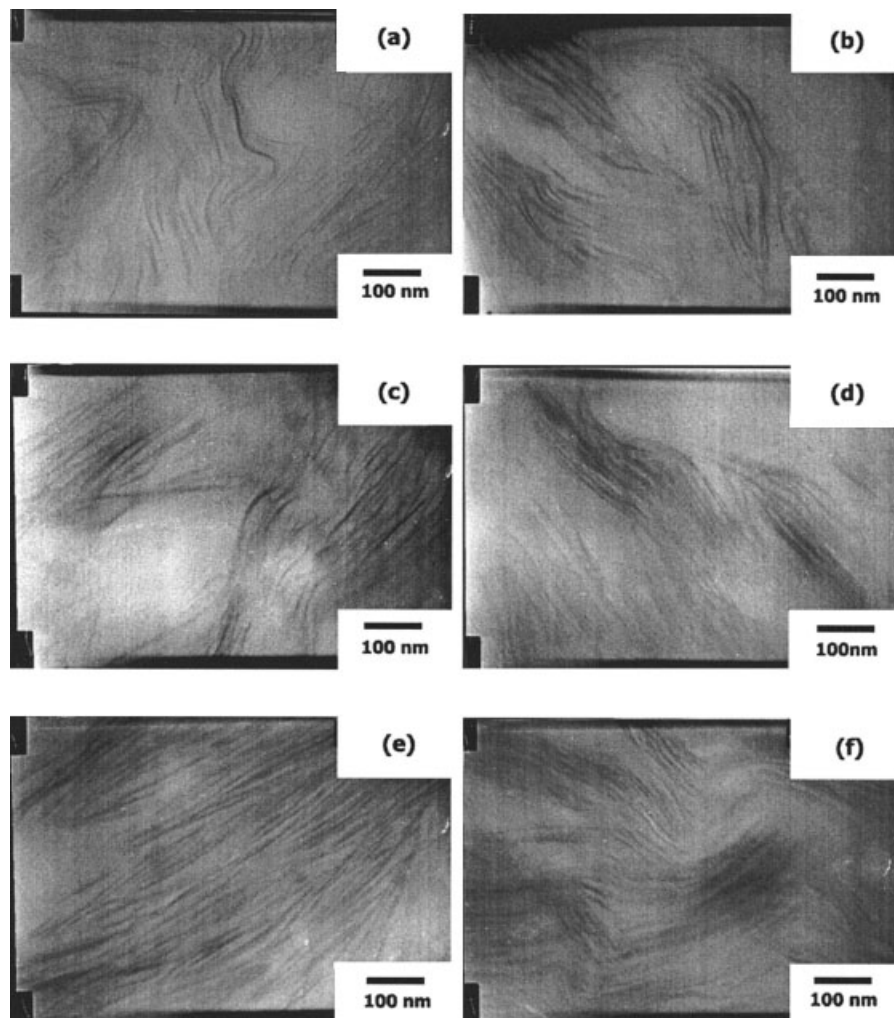


**Figure 4** TEM images of PP/clay nanocomposites, containing 10 wt % clay; (a) P-1, (b) P-3, (c) P-4, (d) P-5, (e) P-6, (f) P-7.

parison with Figure 2, XRD patterns in Figure 3 were very similar to those in Figure 2. This was somewhat unexpected. Generally, the particle's dispersion in the particulate filled PP composites is improved through the additional compounding operation. However, in this clay nanocomposite, no improvement was observed. From this result, it is thought that once the clay

dispersion morphology has been formed in the first compounding step, the dilution of neat PP and the additional shear force exerted in the second compounding step doesn't affect the clay dispersion. This might be caused by the inherent polarity difference between neat PP and PPgMA/clay master batch composites.

**TABLE II**  
Mechanical Properties of PP/Clay Nanocomposites Prepared by a Two-Step Compounding Process<sup>a</sup>

Sample code	Tensile strength (kgf/cm <sup>2</sup> )	Elongation (%)	Flexural modulus (kgf/cm <sup>2</sup> )	Impact strength (kgf-cm/cm)	Shrinkage (‰)
P-1	333	10	22800	4.2	7.0
P-2	—	—	—	—	—
P-3	265	10	19000	4.0	9.5
P-4	275	20	19500	4.5	9.0
P-5	280	30	19800	5.0	9.5
P-6	290	42	20500	6.0	8.5
P-7	295	12	21000	4.1	8.5
PP/talc	255	44	17060	7.0	13

<sup>a</sup> All samples have the same density, 0.940 g/cm<sup>3</sup>.

**TABLE III**  
**Compounding Formulations of Waist Line Molding and Cowl Top Cover Prepared Using PP/Clay Nanocomposites and Their Mechanical Properties**

Properties	Waist line molding		Cowl top cover	
	Conventional PP-talc composite	Clay nanocomposite	Conventional PP-talc composite	Clay nanocomposite
Formulation (wt %)	Block-PP : 60 POE : 15 Talc : 35	MB-7 : 35 POE : 20 Block-PP : 45	Block-PP : 60 Talc : 40	MB-7 : 50 POE : 5 Block-PP : 45
Inorganic content (wt %)	35	9.2	40	13.2
Melt index (g/10 min)	8	2.4	7	0.2
Density (g/cm <sup>3</sup> )	1.12	0.975	1.25	1.01
Tensile strength (kgf/cm <sup>2</sup> )	200	273	270	304
Elongation (%)	20	15	10	8
Flexural modulus (kgf/cm <sup>2</sup> )	14,000	22,570	35,000	33,150
Impact strength (kgf-cm/cm)	6.5	5.6	4	3.2
Shrinkage (‰)	5.0	4.0	8.0	5.6

Figure 4(a–f) show TEM images of formulation code, P-1 to P-7, which were prepared by a two-step compounding process. For samples P-1 and P-7, PH-200 was used for these two composites. The weight ratio of compatibilizer to clay is 2.3 in sample P-1 and 1.5 in sample P-7. Figure 4(a) shows that the particles of silicate layers were dispersed at the nanometer level. Each layer of the clay was dispersed homogeneously in the PP matrix. On the other hand, there were some aggregates of the clay layers at the micrometer level in Figure 4(f). This was because the ratio of compatibilizer to clay in Figure 4(a) was higher than that in Figure 4(f).

### Mechanical properties

Table II summarizes the mechanical properties of PP nanocomposites prepared by a two-step compounding process and neat block-PP/talc microcomposite, which contains 7 wt % talc. It is noteworthy that the tensile strength and flexural modulus of P-1 were about 1.3 times higher than that of neat PP/talc microcomposite. The role of the clay as a reinforcement in the nanocomposite was evident. And the shrinkage property of clay nanocomposites showed the large decreased values compared with that of conventional PP/talc microcomposite. This result showed one of the important structural advantages of clay nanocomposites. For the application of particulate filled polymeric materials to automotive large vehicle parts, low shrinkage and low linear thermal expansion are key factors for dimensional stability. For this purpose, clay nanocomposites are expected to be the most suitable material. Another important property for automotive parts, impact strength of clay nanocomposites, was measured. The impact strength values of clay nanocomposites were lower than that of neat PP/talc microcomposite. This was due to the unavoidable addition of lower molar mass of compatibilizer for clay

exfoliation. In other words, a large portion of low molar mass compatibilizer formed a matrix phase together with neat PP. Generally, PPgMA is prepared by the process of free radical maleic anhydride grafting onto PP backbone chain. During this process, PP chain scission is accompanied; consequently, the lower molar mass of corresponding PPgMA is produced. High content of such an oligomer in the composite can adversely affect impact performance. Moreover, incompatibility problems between matrix PP and PPgMA could arise at this high maleic anhydride content of compatibilizer. So moderate maleic anhydride content and higher compatibilizer molar mass would be required to improve the toughness/stiffness balance of such composites.

For the real application of clay nanocomposites for automotive parts, we made two automotive parts, i.e., waist line molding and cowl top cover, using PP/clay nanocomposites. Table III shows the formulation recipes and mechanical properties of conventional PP/talc microcomposites and new clay nanocomposites. New clay nanocomposites' formulation recipes were attained through various compounding and mechanical testings. Figures 5 and 6 show the images of injection-molded waist line molding and cowl top cover. Compared with conventional talc added composites, clay nanocomposites showed the improvements in tensile strength and flexural modulus as well as low shrinkage, one of the key factors in dimensional stability and an essential factor used to manufacture large vehicle parts, although smaller amount of inor-

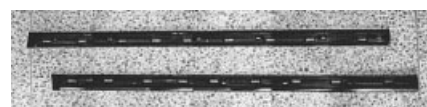


**Figure 5** Image of injection-molded waist line molding prepared by using PP/clay nanocomposite.



**Figure 6** Image of injection-molded cowl top cover prepared by using PP/clay nanocomposite.

ganic material were used. However, impact property was lower than that of conventional PP/talc composites. This weak mechanical property of PP/clay nanocomposite is expected to be improved by controlling the properties of compatibilizer.

### CONCLUSIONS

In this work, PP/PPgMA/clay nanocomposites were prepared by a two-step melt compounding process and two automotive parts were made using these clay nanocomposites. The clay's dispersion morphology was determined in the first compounding step and the dilution of neat PP and additional shear force exerted in the second compounding step didn't influence the clay exfoliation. For the effective continuous operation of twin-screw extruder compounding processing, it was necessary to use PPgMA with medium molecular weight and moderate degree of maleic anhydride grafting. Strength and stiffness increased with the extent of clay exfoliation, but impact resistance decreased. This reduction in toughness was attributed to the addition of lower molar mass PPgMA to exfoliate clay layers. On-going research is aimed at the effect of high molar mass PPgMA on impact property and clay exfoliation. PP/clay nanocomposites will be a new class of particulate filled polymeric composites with unique mechanical properties and offer advantages on density and processing with respect to polymeric composites currently used in the automotive parts fabrication.

### References

1. Vaia, R. A.; Jandt, K. D.; Kramer, E. J.; Giannelis, E. P. *Chem Mater* 1996, 8, 2628.
2. Wu, Z. G.; Zhou, C. X.; Qi, R. R.; Zhang, H. B. *J Appl Polym Sci* 2002, 83, 2403.
3. Tyan, H. L.; Liu, Y. C.; Wei, K. H. *Polymer* 1999, 40, 4877.
4. Frohlich, J.; Thomann, R.; Mulhaupt, R. *Macromolecules* 2003, 36, 7205.
5. Usuki, A.; Kato, M.; Okada, A.; Kurauchi, T. *J Appl Polym Sci* 1997, 63, 137.
6. Kawasumi, M.; Hasegawa, N.; Kato, M.; Usuki, A.; Okada, A. *Macromolecules* 1997, 30, 6333.
7. Hasegawa, N.; Kawasumi, M.; Kato, M.; Usuki, A.; Okad, A. *J Appl Polym Sci* 1998, 67, 87.
8. Marchant, D.; Jayaraman, K. *Ind Eng Chem Res* 2002, 41, 6402.
9. Sun, T.; Garces, J. M. *Adv Mater* 2002, 14, 128.
10. Galgali, G.; Ramesh, C.; Lele, A. *Macromolecules* 2001, 34, 852.
11. Reichert, P.; Hoffmann, B.; Bock, T.; Thomann, R.; Mulhaupt, R.; Friedrich, C. *Macromol Rapid Commun* 2001, 22, 519.
12. Ellis, T. S.; Angelo, J. S. *J Appl Polym Sci* 2003, 90, 1639.
13. Gu, S.; Ren, J.; Wang, Q. *J Appl Polym Sci* 2004, 91, 2427.
14. Wang, Y.; Chen, F.; Wu, K. *J Appl Polym Sci* 2004, 93, 100.
15. Li, J.; Zhou, C.; Gang, W. *Polym Test* 2003, 22, 217.
16. Li, J.; Zhou, C.; Wang, G.; Zhao, D. *J Appl Polym Sci* 2003, 89, 3609.
17. Hasegawa, N.; Okamoto, H.; Kato, M.; Usuki, A. *J Appl Polym Sci* 1918, 2000, 78.
18. Tang, Y.; Hu, Y.; Wang, S.; Gui, Z.; Chen, Z.; Fan, W. *J Appl Polym Sci* 2003, 89, 2586.
19. Liu, X.; Wu, Q. *Polymer* 2001, 42, 10013.
20. Hasegawa, N.; Usuki, A. *J Appl Polym Sci* 2004, 93, 464.
21. Lopez, M.; Valle, M.; Sapunar, R.; Quijada, R. *J Appl Polym Sci* 2004, 92, 3008.
22. Silva, A.; Rocha, M.; Countinho, F.; Bretas, R.; Scuracchio, C. *J Appl Polym Sci* 2001, 79, 1634.
23. Silva, A.; Tavares, M.; Politano, D.; Countinho, F.; Rocha, M. *J Appl Polym Sci* 2005, 1997, 66.
24. Silva, A.; Rocha, M.; Countinho, F.; Rocha, M.; Countinho, F.; Bretas, R.; Scuracchio, C. *J Appl Polym Sci* 2000, 75, 692.
25. Kontopoulou, M.; Wang, W.; Gopakumar, T.; Cheung, C. *Polymer* 2003, 44, 7495.
26. Carriere, C.; Silvis, H. *J Appl Polym Sci* 1997, 66, 1175.
27. Godail, L.; Packham, D. *J Adhesion Sci Technol* 2001, 15, 1285.
28. Annual Book of ASTM Standards 1988. (08-01)-Plastic-C(1)-2343.